



Experimental and Numerical Analysis of the Behaviour of Padauk Wood under Thermal Aggression

Desmond Mufor-Zy¹, Jean Aimé Mono¹, Armand Fopah-Lele^{2*}

¹Laboratory of Forest and Wood Resource Development (LaReFob), Higher Technical Teacher's Training College (ENSET), University of Douala, Cameroon

²Department of Mechanical Engineering, Faculty of Engineering and Technology, University of Buea, P.O. Box 63, Buea, Cameroon

*Corresponding author, Email address: a.fopah-lele@ubuea.cm

Received 24 July 2022,
Revised 28 Aug 2022,
Accepted 29 Aug 2022

Keywords

- ✓ Padauk wood,
- ✓ thermal constraint,
- ✓ finite element model,
- ✓ thermal behaviour,
- ✓ numerical modelling.

a.fopah-lele@ubuea.cm
Phone: +237 673321855;

Abstract

Timber is combustible but considered as a building material that has acceptable benefits due to its high strength and stiffness to weight ratios, environmentally friendly, and excellent for furniture design and production of wood-based materials. As timber is combustible, thermal aggression might be an issue for the deployment of timber usage in building structures for example. The heat treatment of the material at high temperatures can be used to improve dimensional stability and increase durability and resistance to biological degradation like fungi attacks. This article aims at describing an experimental investigation on the behavior of padauk wood under thermal aggression. The investigation of padauk wood was processed and thermophysical characterized. Thirty-five (35) padauk woods with different numbers, lengths, widths, and thicknesses were characterized under high temperatures (103 °C, 150 °C, 200 °C, and 250 °C) to observe effects on thermal effusivity, specific heat capacity, thermal conductivity, and thermal diffusivity. This allows a fast, comprehensive, and realistic model to be implemented. For that reason, a 1D Quadrupole modeling for a Semi-Infinite and Complete Model was developed using the Laplace transform and validated. The thermal model implicitly considered the upward flow of temperature of the timber. The experimental results obtained regarding the temperature and moisture of padauk wood are compared with the 1D numerical models. Satisfactory agreement (standard deviation of 8%) is obtained during the validation process.

1. Introduction

Timber is an engineering material considered to be excellent for furniture design, production of wood-based materials and construction of modern buildings [1]. Recently, the design and construction of medium and high-rise timber buildings with structural components composed of engineered timber products have significantly increased [2]. These buildings gained popularity as timber presents many advantages due to its high strength and stiffness to weight ratios, biodegradation and its environmental qualities [2–6]. Despite its advantages and sustainability credentials, timber is combustible and presents special thermal safety challenges as compared with concrete and steel neither of which is without its own challenges [7].

Thermal aggression on wood is a concern in the case of building construction and infrastructures with wood structures. It actually consists of a combination of active and passive protection, including means that prevent or slow the spread of smoke and flames [4,8,9]. In order to integrate a product in the field of engineering, the products should meet relevant requirements for structural safety, quality of life,

energy efficiency, cost, durability, must satisfy technical approvals, including thermal resistance tests, which are experimentally assessed in accredited laboratory furnaces [8,10]. Researchers have shown that the behaviour of wood is predictable under thermal exposure. Several works such [7,11–15], have provided design strategies to determine the thermal resistance-engineered timber structures based on a simplified reduced cross section calculation methodology. Indeed, combustion of wood is slow and char is generated on its surface, which acts as insulation and protects the inner core materials. Nevertheless, the combustion on the surface reduces the effective size of the cross section at the same time. The wood charring rate is important with regard to the density, oxygen permeability, moisture content, geometric size and other various factors [16]. The process validation of a product regarding a thermal resistance test is very complex and this is a bottleneck to any innovation. In this context, the use of simulation tools may offer an alternative to real thermal resistance tests in determining the thermal resistance behaviour of a product, for instance during preliminary design stages. The approach of a “Virtual Furnace” is therefore being developed in some laboratories in order to model a thermal resistance test [17]. The scientific approach consists of coupled simulation of (i) the gas temperature and flux (using computational fluids dynamics software) and (ii) the thermal behaviour of the structure (most often carried out with finite element solvers). Such a tool mimics virtually the thermal behaviour of the tested product when it is exposed to a standard thermal impulsion in a laboratory furnace. Using a “Virtual Furnace” allows better analysis and evaluation of a large number of technical alternatives, before a conclusive thermal resistance test is carried out. Moreover, numerical simulations may improve the testing conditions, including heating power (control of the furnace) and metrology [8]. Timber is the structural material for which the studies on the properties and the tools of simulation in thermal situations are the least numerous. The large variety of wood species and the natural origin of the material, leading to a large variability of its characteristics, makes difficult the synthesis of the data and the development of generalized models [3]. Commercial tropical timber species, especially in Cameroon, such as Iroko (*Milicia excelsa*) and Padauk (*Pterocarpus soyauxii Taub*) possess increasing demand in various wood products applications that requires developing modern timber processing technologies. Padauk has excellent decay resistance and is rated as a durable to very durable species [1]. It is also resistant to termite attacks and of another type of insect attack.

In the thermal research field, several studies are available on the behaviour of solid wood under exposure to fire. The reason for this being the widespread use of wood as a structural product in constructions (timber) for example. Nevertheless, large limitation still exist due to the lack of data, especially in a tropical use conditions such as in Cameroon. Thus, the design rules developed are based particularly on a limited number of experimental and numerical results. This is due to high cost of large-scale experiments in thermal conditions and the complexity to develop accurate numerical models. Based on the observation, a specific research project was carried out on thermal characterization of commercial tropical timber species padauk wood (*Pterocarpus soyauxii Taub*) in Cameroon, aiming to understand the thermal behaviour of padauk, allowing the particularities of each specimen at different temperature to be taken into account. While, African padauk is considered as a durable wood with superior physical and mechanical properties and may not need additional characterization, nevertheless, thermal treatment may render colour homogeneity to the wood due to chemical changes, expand and contract with varying temperature due to varying moisture content. This paper aims at describing an experimental and numerical investigation on the behaviour of padauk wood under thermal aggression. Although there are recent developed numerical tools [18,19], a 0D based model if first developed in order to understand and validate the built-in experiment at the lab disposal.

In this paper, the results of the experimental and numerical investigations on the thermal behaviour of padauk wood are presented. First, a numerical model based on Laplace Transform failure criterion is presented to simulate the orthogonal anisotropy behaviour of padauk. The experimental results used to validate the numerical models in thermal conditions are presented. Then, two successive modelling stages are described: first, a 1D asymmetric semi-infinite hot plane model with heat transfer inside at the centre components and, secondly, the asymmetric 1D Quadrupole Models for the Complete Model. At each stage, the numerical results are compared with the experimental data. This comparison allows for the validation of the numerical approach discussed in this paper.

2. Methodology

2.1 Sample preparation

The present study uses defect free commercial tropical padauk wood samples (*Pterocarpus soyauxii* Taub) of dimensions 100mm long, 100mm wide, and 30mm thick. A wood depot in the Littoral Region of Cameroon (Figure 1) supplied it. The samples were dehydrated in an oven at 103 °C for more than 48 h to remove moisture content. Their mass was monitored every 2 h during the drying process to ensure mass stabilization. The samples were then sealed in plastic bags. Later, it was weighted again after cooling, to ensure that any change in the moisture content was insignificant.



Figure 1. Wood samples used for the characterization of thermal properties at high temperatures

2.2 Experimental characterization

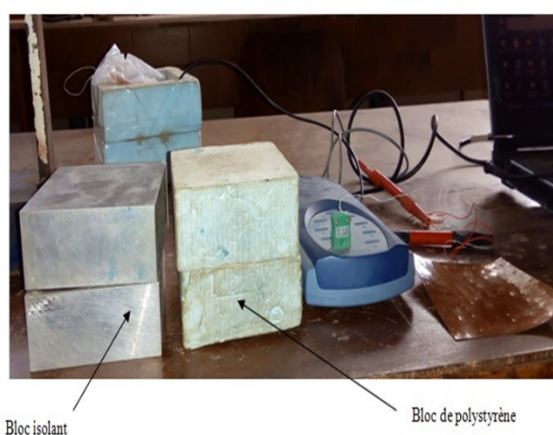
The experimental studies in this paper were carried out at Pycnolab[®] Sarl in Douala and at the Mechanical Laboratory of the National Advanced School of Engineering (ENSP) Yaoundé in Cameroon. Thirty-five (35) padauk wood samples were tested under different temperatures to investigate their thermal behaviour and to validate the aforementioned numerical model. The characterization of the samples was carried out in 3 phases. The temperature profile and phases are shown in Table 1. In phase 1, the wood samples were heated up to the desired final temperature (150 °C, 200 °C, and 250 °C). In Phase 2, the desired temperature was maintained for 3 h. In phase 3, the samples were gradually cooled down and re-moistened to achieve a moisture content in the range of 9.25–10.92%. Before testing, all the specimens were stored and conditioned at normal room temperature (25 °C) and humidity for 3h.

Table 1. Conditions and parameters of thermal modification process used in this study

Parameters	Thermal Modification Schedule			
	103 °C	150 °C	200 °C	250 °C
Heating time (h)	0	10	13.5	19.1
Modification time (h)	3	3	3	3
Cooling time (h)	0	3	5.3	6.1
Total time (h)	3	16	21.8	28.2

2.3 Experimental setup

The device used for the experimental setup consists of a simple heating resistor "MINCO 230Ω P" placed between two flat surface samples of the wood sample to be characterized. The heating element (probe) and the sample have preferably the same surface, in order to be able to make the hypothesis that the heat transfer is unidirectional during the time, while the convective lateral losses are negligible. **Figure 2** shows the used block to force heat transfer in one direction. A thermocouple of type K is placed on the face of the resistor in contact with the sample. The thickness of the sample is carefully selected so that the semi-infinite medium assumption for the sample is verified for at least a few seconds. A heat flux step (thermal power $P=UI$) is also applied by means of a power generator (stabilized between 0-30 V) and the temperature evolution $T_s(t)$ at the centre of the heating element is recorded by means of the *Picolog* probe. When perturbation has not reached the other faces, it is considered that the heat transfer at the centre of the sample is unidirectional. The experimental setup is as shown in **Figure 3**.

**Figure 2.** Polystyrene block and insulating block**Figure 3.** Asymmetrical hot plane experimental device

2.4 Thermal characterization

Thermal properties at different temperatures were measured using the thermophysical characterization method. This method is a technique for measuring the volume heat capacity ρC_p and thermal effusivity E and building materials in transient. Four pairs of samples dimensioned 100mm long, 100mm wide, 30mm thick cut from the same board were tested. Before test, samples were dehydrated in an oven at 103 °C for at least 48 h in order to remove water content without degrading samples. Their mass was monitored every 2 hours during the drying process to ensure mass stabilization. The samples were then sealed in plastic bags and weighted again after cooling. The mean thermal conductivity is 0.1823 W/m·K with quite a low standard deviation. This underlines the

homogeneous measurements for each sample. The specific heat capacity of the material that depends on the temperature and moisture content is more variable and varied slightly between different temperatures. This was comparable with the thermal properties of solid wood from literature [20–22].

2.5 Numerical modelling

a) 1D Quadrupole Modelling for a Semi-Infinite Model

The quadrupole method is a well-known analytical tool in heat transfer modelling. It is a precise method to predict temperature in time-varying linear systems [23] based on finite element principle [24]. With the temperature at the centre of the probe, the asymmetric hot plane model shown in **Figure 4** is considered. The transverse dimensions of the resistor being large compared to the thickness of the sample, it is considered that the heat transfer remains unidirectional at the centre of the probe and models it using the quadrupole method. In this case, the lateral convective losses h at the lateral faces of the sample is neglected. In a second step, the heating element (probe) is assumed as a thin system (the temperature will then be uniform over the entire thickness of the probe).

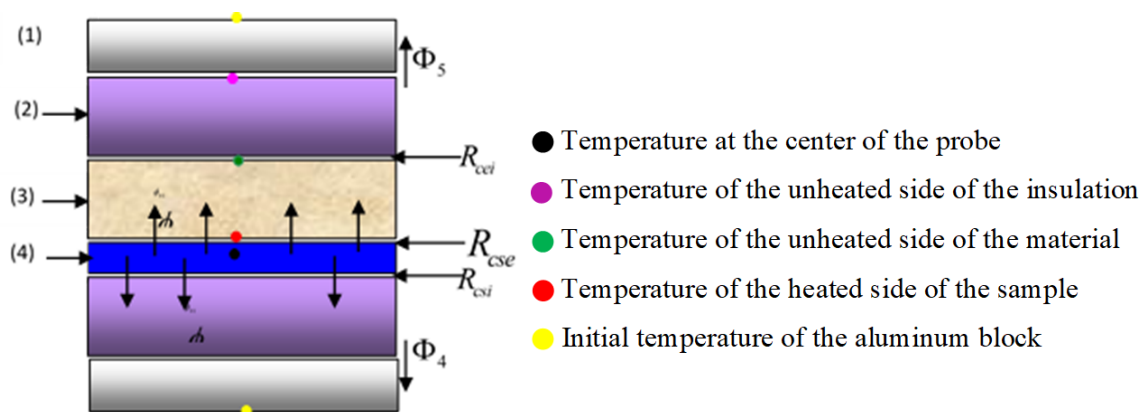


Figure 4. Hot plane experimental setup view (Front view of the symmetrical hot plane experimental setup).

Figure 4 describes the heat transfer phenomena occurring during this experiment, where : (1) Aluminium block; (2) insulating material; (3) sample to be characterized; (4) heating resistor, R_{cse} is the contact resistance at the probe/sample interface, R_{cei} is the contact resistance at the sample/insulator interface, and R_{csi} is the contact resistance at the probe/insulator interface.

The thermal quadrupole method applied to the sample for the upward flow is written as follows:

$$\begin{pmatrix} \theta_0 \\ \Phi_{01} \end{pmatrix} = [M_1][M_2][M_3] \quad \text{Eqn. 1}$$

$\theta_0 = L(T_0(x, t))$ is the Laplace transform of the temperature rise at the heating element (probe).

$\Phi_{01} = L(\phi_0(x, p))$ is the Laplace transform of the heat flux density dissipated in the sample upwards.

M_1 is the element representing the half thickness of the probe:

$$[M_1] = \begin{pmatrix} 1 & 0 \\ \frac{m_s c_s}{S} p & 1 \end{pmatrix} = \begin{pmatrix} 1 & 0 \\ \rho_s c_s e_s p & 1 \end{pmatrix} \quad \text{Eqn. 2}$$

M_2 is the element representing the contact resistance at the probe-sample interface:

$$[M_2] = \begin{pmatrix} 1 & SR_{cse} \\ 0 & 1 \end{pmatrix} \quad \text{Eqn. 3}$$

M_3 is the element representing the material considered as semi-infinite:

$$[M_3] = \begin{pmatrix} \theta_3 \\ E\sqrt{p}\theta_3 \end{pmatrix} \quad \text{Eqn. 4}$$

The quadrupole method applied for the downward flow is given when also considering the insulator as a semi-infinite material:

$$\begin{pmatrix} \theta_0 \\ \Phi_{02} \end{pmatrix} = [M_4][M_5] \quad \text{Eqn. 5}$$

Φ_{02} is the Laplace transform of the heat flux density dissipated in the sample downwards. M_4 is the element representing the contact resistance at the probe-insulator interface:

$$[M_4] = \begin{pmatrix} 1 & SR_{csi} \\ 0 & 1 \end{pmatrix} \quad \text{Eqn. 6}$$

M_5 is the element representing the insulating material considered as semi-infinite:

$$[M_5] = \begin{pmatrix} \theta_4 \\ E_i\sqrt{p}\theta_4 \end{pmatrix} \quad \text{Eqn. 7}$$

The following relation gives the total flux density:

$$\phi_0 = \phi_1 + \phi_2 \quad \text{Eqn. 8}$$

Combining all these different matrices lead the relation that represents the theoretical response of the asymmetric semi-infinite hot plane model in Laplace space:

$$\theta_c(x, p) = \frac{\phi_0 S}{p} \cdot \frac{1}{\frac{\rho_s c_s e_s S p + (1 + R_{chs} \rho_s c_s e_s S p) E S \sqrt{p}}{1 + R_{chs} E S \sqrt{p}} + \frac{E_i S \sqrt{p}}{1 + R_{chi} E_i S \sqrt{p}}} \quad \text{Eqn. 9}$$

$\theta_0(x, p)$ is the Laplace transform of the temperature at the centre of the probe at $T_s(t) = T_0(t) - T(0)$. A simplified estimation at a longer time (simplified model) of the relation in **Eqn. 9** allows obtaining in real space the temperature distribution:

$$\Delta T(0, t \rightarrow \infty) = \phi_0 S \left(\frac{E^2 R_{chs} + E_i^2 R_{chi}}{(E + E_i)^2} - \frac{\rho_s c_s e_s}{S(E + E_i)^2} \right) + \frac{2\phi_0}{(E + E_i) \cdot \sqrt{\pi}} \sqrt{t} \quad \text{Eqn. 10}$$

The numerical calculation of the slope α of curve $T=f(t/2)$, which thus allows to obtain a pre-estimate (*preest*) of the thermal effusivity of the material given by the relation in **Eqn. 11**.

$$E_{preest} = \frac{2\phi_0}{\alpha\sqrt{\pi}} - E_i \quad \text{Eqn. 11}$$

The volumetric heat capacity ρC_p can also be pre-estimated from the simplified model. The heat transfer δq through the probe during an dt infinitesimally small time interval corresponds to a heat flow $\rho_0 = \delta q/dt$, which causes a temperature rise dT in the probe. By exploiting the linear part of the thermograms $T=f(t)$, its slope β can be calculated numerically and thus the pre-estimated value of the volume heat capacity of the sample can be deduced by the relation:

$$(\rho C_p)_{preest} = \frac{\phi_o - \rho C_{pi} e_i - \rho C_{ps} e_s}{e} \quad \text{Eqn. 12}$$

The pre-estimates of E and ρC_p will allow us to determine the apparent thermal conductivity of the materials by the relation in **Eqn. 13**.

$$\lambda_{preest} = \frac{(E^2)_{preest}}{(\rho C_p)_{preest}} \quad \text{Eqn. 13}$$

b) Symmetric 1D Quadrupole Model for the Complete Model

Symmetries play a pivotal role in understanding various topological phases of matter. Looking for analytical relationships between temperature and heat flux at some given locations is necessary. With the temperature sensor at the centre of the probe, the diagram in **Figure 2** still holds. Applying the quadrupole formalism [25], the following equations can be written:

$$\begin{pmatrix} \theta_0 \\ \Phi_{01} \end{pmatrix} = [M_1][M_2][M_6][M_7][M_8] \begin{pmatrix} \theta_5 \\ \Phi_5 \end{pmatrix} = \begin{pmatrix} A & B \\ C & D \end{pmatrix} \begin{pmatrix} \theta_5 \\ \Phi_5 \end{pmatrix} \quad \text{Eqn. 14}$$

M_6 is the element representing the material to be characterized:

$$[M_6] = \begin{pmatrix} A_e & B_e \\ C_e & D_e \end{pmatrix} \quad \text{Eqn. 15}$$

With:

$$A_e = \cosh(q_e \cdot e) \quad B_e = \frac{\sinh(q_e \cdot e)}{\lambda_e \cdot q_e} \quad \text{Eqn. 16}$$

$$C_e = \lambda_e \cdot q_e \cdot \sinh(q_e \cdot e) \quad D_e = A_e$$

M_7 is the element representing the contact at the sample/insulator interface:

$$[M_7] = \begin{pmatrix} 1 & SR_{cei} \\ 0 & 1 \end{pmatrix} \quad \text{Eqn. 17}$$

M_8 is the element representing the insulating material:

$$[M_8] = \begin{pmatrix} A_i & B_i \\ C_i & D_i \end{pmatrix} \quad \text{Eqn. 18}$$

With:

$$A_i = \cosh(q_i \cdot e_i) \quad B_i = \frac{\sinh(q_i \cdot e_i)}{\lambda_e \cdot q_i} \quad \text{Eqn. 19}$$

$$C_i = \lambda_i \cdot q_i \cdot \sinh(q_i \cdot e_i) \quad D_i = A_i$$

The role of the aluminium block here is to maintain constant the temperature at the interface insulating material/aluminium block. The evaluation of the *Biot* number for this block is done through the equation **Eqn. 20**:

$$(Bi)_{bloc} = \frac{h_{bloc} \cdot b}{\lambda_{bloc}} \quad \text{Eqn. 20}$$

With the values $h_{bloc}=10\text{W/m}^2\text{K}$; $\lambda_{bloc} = 200 \text{ W/m}\cdot\text{K}$, $b=100\text{mm}$, $Bi=0.005$, which is much lower than 0.1, in this case it is considered uniform. Let then set its boundaries:

$$\begin{aligned}\theta_3(x, p) &= L(\Delta T(x, p))_{bloc} = 0 \\ \theta_4(x, p) &= L(\Delta T(x, p))_{bloc} = 0\end{aligned}\tag{Eqn. 21}$$

Similarly, in the specific heat capacity equation, the matrix element M_8 replaces the matrix M_5 , i.e.:

$$\begin{pmatrix} \theta_0 \\ \Phi_{02} \end{pmatrix} = [M_4][M_8] \begin{pmatrix} \theta_4 \\ \Phi_4 \end{pmatrix}\tag{Eqn. 22}$$

By combining relations **Eqn. 1**, **Eqn. 11** and **Eqn. 19**, the temperature at the center of the probe in Laplace space was found, given by relation in **Eqn. 23**:

$$\theta_0(x, p) = \frac{\phi_0}{p} \cdot \frac{1}{\frac{D}{B} + \frac{D_i}{B_i + R_{csi}D_i}}\tag{Eqn. 23}$$

The Levenberg-Marquart algorithm [26] integrated in a Matlab code then allows estimating the value of E that minimizes the sum of the squared deviation errors of the functional ψ between experimental and theoretical curves. This leads to the following equation:

$$\psi = \sum_{i=1}^n [\Delta T_{\text{exp}}(t_i) - T_{\text{model}}(t_i)]^2\tag{Eqn. 24}$$

3. Results and Discussion

The samples were oven-dry to remove all humidity from their interior, and consequently to avoid all the influences of humidity in the measured values. After that, the samples were exposed to humid air. Equilibrium condition for wood specimens were considered. Temperature readings were taken at six various points as shown in **Figure 4** at a time interval of hour to generate a temperature profile along the time of carbonisation. The initial set of temperature measurements was done right at the ignition and the final set was done when the system had come into thermal equilibrium.

3.1 Thermal modification diagram

Despite appearing to be a solid material, the samples were made up of atoms that are far from stationary.

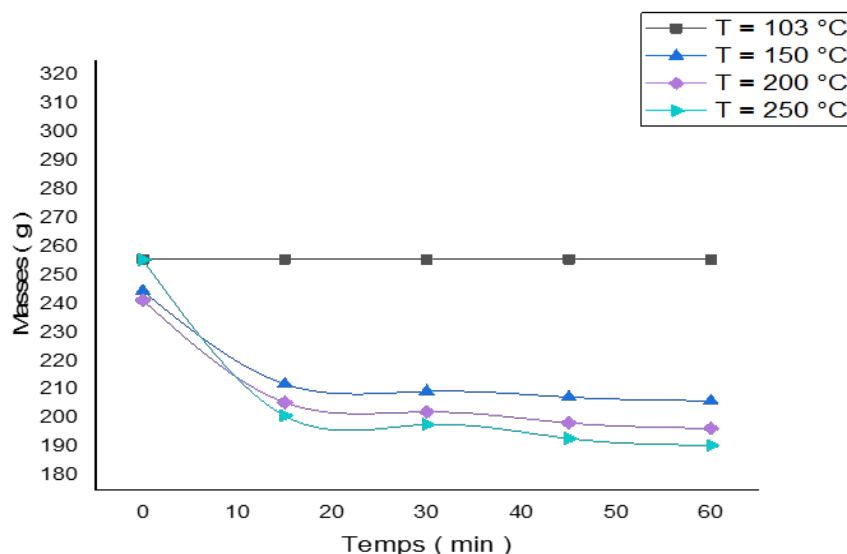


Figure 5. Thermal Modification graph

When the samples were exposure to different temperatures within different timeframe in an oven, the wood was electrically insulating causing the movement speed of these components increases, hastening internal reactions. On Figure 5, as moisture content increases, however, electric conductivity increases such that the behaviour of saturated wood (wood with maximum moisture content) approaches that of water and, it was notice that moisture reduces the heating value of the wood samples. As such, the sample at 103 °C had the least heating value while 250 °C had the highest heating value and as temperature increase or decreases so does its ability to hold water as shown in Figure 5. When the temperature was raise to 250 °C a spark or flame ignited it indicating that if temperature was raise above 250 °C to about 500 °C ignition is spontaneous.

3.2 Experimental results

Figure 6 highlights the evolution of the experimental temperature in the centre of the wood material, conditioned at different temperatures. A good correlation between the experimental results and these thermograms can be seen. The thermal conductivity of these woods increases as their temperature increases. This may be because, when the material is heated, water evaporates as it is heated, but the wood material tends to gradually crack, leaving "channels" for the rapid passage of heat, and thus contributes to increasing their thermal conductivity. Contrary to the earth/sand material where the arrangement of the aggregates creates internal pores within the agglomerated material, the latter then traps the air (of very low conductivity $0.026 \text{ Wm}^{-1}\text{K}^{-1}$) thus making heat transfer difficult within the material. This is not the case for the wood material, hence the strong dependence of the thermal conductivity on the temperature.

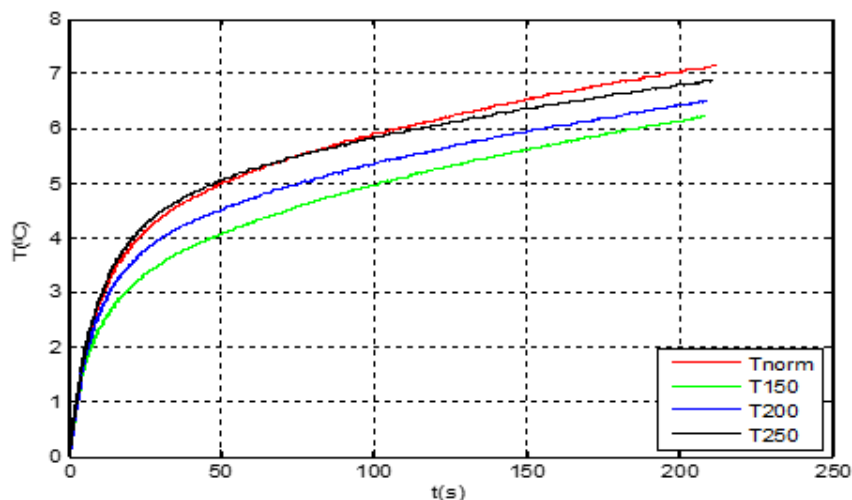


Figure 6. Evolution of the temperature at the centre of the samples as a function of time

3.3 Numerical results

The analysis of the reduced sensitivities curves shows clearly that the parameters E and ρC_p are not correlated (Figure 7). Contrary to the thermograms obtained by the simplified model where this model does not allow a minimization of the sum of the quadratic deviations between thermograms T_{exp} and thermograms T_{mod} , we notice that the complete model minimizes the deviations between these two thermograms (they are perfectly superpose in Figure 8a). This is even more justified by the observation of their residual curves: green curve (Figure 8b), they are perfectly centred (with a little bias at the beginning of the sample. The material being rigid requires some seconds before the heat flux starts to propagate to the centre.

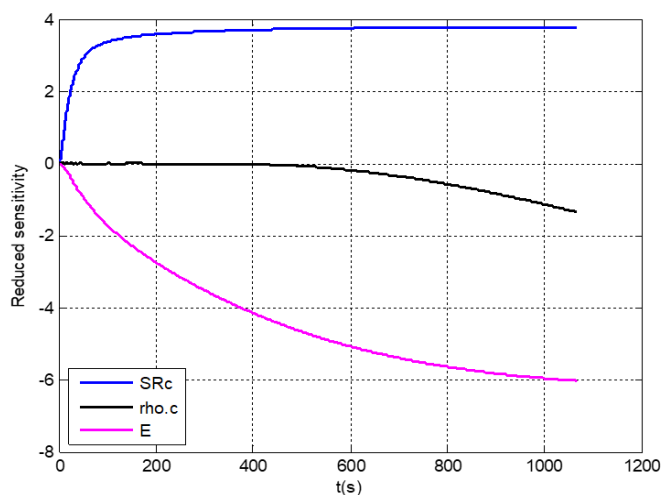


Figure 7. Reduced sensitivity curve: Sample T_1

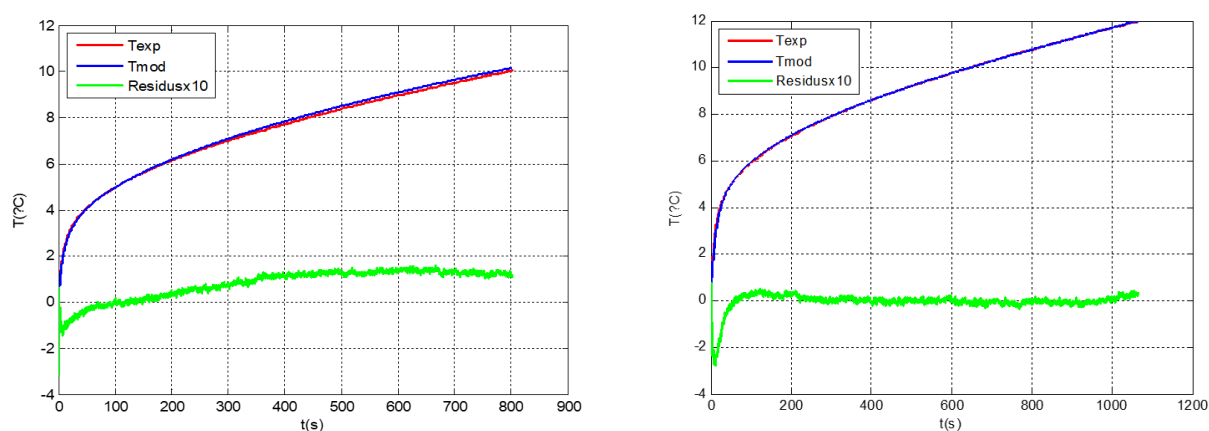


Figure 8. a. Thermogram of temperature $T=f(t)$ obtained from the complete model for sample T_1 sample **b.** Thermogram of temperature $T=f(t)$ obtained from the complete model for sample T_3

Conclusion

This paper presented the result of a measurement campaign of thermal conductivity of *padauk* wood species grown in the littoral region of Cameroon. The hot plane thermal technique is used in the present study to measure the thermal conductivity of *padauk* wood material at different elevated temperature levels expected to be reached in practice. Wood thermal treatment was conducted at 103 °C, 150 °C, 200 °C and 250 °C in a high temperature oven. A 1D numerical model was then developed to validate the experimental results in terms of ambient and thermal tests. The 1D numerical model for sequentially coupled heat–structure analysis was implemented in MATLAB software using the Laplace Transform failure criterion. The following conclusions can be drawn:

- The temperatures on the wood surface are considerably higher than in the core of the wood. The surfaces of the samples achieved the highest temperature, whereas the inner parts did obtain the lowest temperature. The temperatures on the wood surface can achieve the target temperature within a short time, the lengths of time required for the samples to be treated at 103 °C, 150 °C, 200 °C, and 250 °C, respectively, were as follows: 0, 15, 30, 45 and 60 minutes.
- For the relationship between wood central point temperatures or moisture content, treatment time, and treatment medium temperatures, a generator was use. It was use to predict wood temperatures at the central point during wood thermal treatment at 103 °C, 150 °C, 200 °C, and

250 °C at different times by diffusing a thermal power to the centre of the probe and the temperatures are recorded via a thermocouple.

- After the thermal treatment of the samples at different temperatures, it was noticed that the higher the temperature, the darker the surface of the wood become. When the temperature was raised to 250 °C a spark or flame was ignited indicating that above that temperature ignition could be spontaneous. A strong odour could be gotten from the samples when exposed to temperature and the higher the temperature, the stronger the odour.
- Results are in line with literature values and, in general, conductivity augments with water content increasing. The relationship between water content and conductivity results linear for the wood samples. Thermal conductivity decreases with increasing density over the temperature and density ranges considered. The increase in conductivity due to increase in temperature is relatively large, while the change due to change in density is relatively small. The thermal conductivities of the samples measured in the “axial” direction differ in general by a substantial amount (about 20%) compared to those measured in the “radial” direction. For the axial direction, increasing density of insulation materials acts in general to decrease the conductivity. The opposite behaviour is obtained for these insulation materials for the radial direction. The results show that increasing density acts to increase the radial thermal conductivity.
- After the development of the numerical simplified model, it was observed that the model allows to estimate E and ρCp . Although, the simplified model in view of the reduced sensitivities curves show that this model allows to estimate E and ρCP , the analysis of the curves shows the contrary. That the obtained results cannot be validated yet, insofar as one observes a non-convergence between the curves of the model (Eqn. 14, curve T_{mod}) and the experimental results model (curve T_{exp}). It is therefore necessary to carry out a study using the complete model.
- After the evolution of the experimental temperature in the centre of the wood material, conditioned at different temperatures (Figure 6), a good correlation between the experimental results and these thermograms can be now observed. The thermal conductivity of these woods increases as their temperature increases. This may be because, when the material is heated, water evaporates as it is heated, but the wood material tends to gradually crack, leaving "channels" for the rapid passage of heat, and thus contributes to increasing their thermal conductivity. Contrary to the earth/sand material where the arrangement of the aggregates creates internal pores within the agglomerated material, the latter then traps the air (of very low conductivity $0.026 \text{ Wm}^{-1}\text{K}^{-1}$) thus making heat transfer difficult within the material. This is not the case for the wood material, hence the strong dependence of the thermal conductivity on the temperature.

The results of this study can be used to devise a wood thermal treatment schedule, understand the heat and moisture distribution, and control the process of wood heat treatment, thus guiding wood thermal treatment to reduce energy and time consumption. This method can also be used to evaluate conditions for wood drying and other wood thermal treatments to simulate and predict heat and moisture content distributions as well as guide other practical production processes. Numerous properties of thermally modified wood, such as dimensional stability, hygroscopic, and mechanical strength, are closely related to the treatment temperature, treatment time, and wood moisture content. Therefore, future study can be completed by characterizing the homogenized thermo-mechanical properties [27] of *padauk* wood to determine the deformed shape of the wood after a certain time of thermal aggression and use the mathematical model developed with the help of COMSOL Multiphysics to simulate heat and mass transfers.

Acknowledgement: This research did not receive any specific grant from funding agencies in the public, commercial, or not-for-profit sectors. Authors acknowledge in advance the editor and reviewer's comments and thank them to their contribution in improving the paper quality.

Disclosure statement: *Conflict of Interest:* The authors declare that there are no conflicts of interest. *Compliance with Ethical Standards:* This article does not contain any studies involving human or animal subjects.

References

- [1] R. Corleto, M. Gaff, P. Niemz, A.K. Sethy, L. Todaro, G. Ditommaso, F. Razaeei, A. Sikora, L. Kaplan, S. Das, G. Kamboj, M. Gašparík, F. Kačík, J. Macků, Effect of thermal modification on properties and milling behaviour of African padauk (*Pterocarpus soyauxii* Taub.) wood, *J. Mater. Res. Technol.* 9 (2020) 9315–9327. <https://doi.org/10.1016/j.jmrt.2020.06.018>.
- [2] Y. Wang, J. Zhang, F. Mei, J. Liao, W. Li, Experimental and numerical analysis on fire behaviour of loaded cross-laminated timber panels, *Adv. Struct. Eng.* 23 (2020) 22–36. <https://doi.org/10.1177/1369433219864459>.
- [3] M. Audebert, D. Dhima, M. Taazount, A. Bouchaïr, Experimental and numerical analysis of timber connections in tension perpendicular to grain in fire, *Fire Saf. J.* 63 (2014) 125–137. <https://doi.org/10.1016/j.firesaf.2013.11.011>.
- [4] Z. He, Z. Wang, L. Qu, J. Qian, S. Yi, Modeling and simulation of heat-mass transfer and its application in wood thermal modification, *Results Phys.* 13 (2019) 102213. <https://doi.org/10.1016/j.rinp.2019.102213>.
- [5] E. Labans, A. Bikovs, K. Kalniņš, FEM Simulation of Mechanical and Thermal Properties of Wood Based Sandwich Panels with Cellular Wood Core, in: *10th Int. Conf. Sandw. Struct. Book Abstr.*, 2012: pp.169–170. <https://ortus.rtu.lv/science/en/publications/15795> (July 24, 2022)
- [6] P. Racher, K. Laplanche, D. Dhima, A. Bouchaïr, Thermo-mechanical analysis of the fire performance of dowelled timber connection, *Eng. Struct.* 32 (2010) 1148–1157. <https://doi.org/10.1016/j.engstruct.2009.12.041>.
- [7] L.A. Bisby, A. Frangi, Special Issue on Timber in Fire, *Fire Technol.* 51 (2015) 1275–1277. <https://doi.org/10.1007/s10694-015-0539-1>.
- [8] G. Cuffe, J.-C. Mindeguia, V. Dréan, D. Breysse, G. Auguin, Experimental and numerical study of the thermomechanical behaviour of wood-based panels exposed to fire, *Constr. Build. Mater.* 160 (2018) 668–678. <https://doi.org/10.1016/j.conbuildmat.2017.11.096>.
- [9] G. Cuffe, J.-C. Mindeguia, V. Dréan, G. Auguin, B. Denys, Thermomechanical behaviour of cellulose-based materials: application to a door under fire resistance test, in: *8th Int. Conf. Struct. Fire, 8th International Conference on Structures in Fire*, Shanghai, China, 2014: p. 9p. <https://doi.org/10.13140/2.1.2247.6169>.
- [10] C. Qi, F. Zhang, J. Mu, Y. Zhang, Z. Yu, Enhanced mechanical and thermal properties of hollow wood composites filled with phase-change material, *J. Clean. Prod.* 256 (2020) 120373. <https://doi.org/10.1016/j.jclepro.2020.120373>.
- [11] A. Barlett, R. Hadden, L. Bisby, A. Law, Analysis of Cross-Laminated Timber Charring Rates upon Exposure to Non-standard Heating Condition, in: *Lond. U. K. Intersci. Commun.*, London United Kingdom: Intersciences Communications, San Francisco, California, USA, 2015: pp. 667–681. <https://espace.library.uq.edu.au/view/UQ:366970> (accessed July 24, 2022).

- [12] M. Klippel, A. Frangi, Fire Safety of Glued-Laminated Timber Beams in Bending, *J. Struct. Eng.* 143 (2017) 04017052. [https://doi.org/10.1061/\(ASCE\)ST.1943-541X.0001781](https://doi.org/10.1061/(ASCE)ST.1943-541X.0001781).
- [13] S.A. Lineham, D. Thomson, A.I. Bartlett, L.A. Bisby, R.M. Hadden, Structural response of fire-exposed cross-laminated timber beams under sustained loads, *Fire Saf. J.* 85 (2016) 23–34. <https://doi.org/10.1016/j.firesaf.2016.08.002>.
- [14] B. Östman, D. Brandon, H. Frantzich, Fire safety engineering in timber buildings, *Fire Saf. J.* 91 (2017) 11–20. <https://doi.org/10.1016/j.firesaf.2017.05.002>.
- [15] J. Schmid, J. König, J. Köhler, Fire-exposed cross-laminated timber—modelling and tests, in: WCTE, Vienna, Austria, 2010: p. 10p.
- [16] J. Zhang, Y. Wang, L. Li, Q. Xu, Thermo-mechanical behaviour of dovetail timber joints under fire exposure, *Fire Saf. J.* 107 (2019) 75–88. <https://doi.org/10.1016/j.firesaf.2017.11.008>.
- [17] L.Y. Cooper, J.-M. Franssen, A basis for using fire modeling with 1-D thermal analyses of partitions to simulate 2-D and 3-D structural performance in real fires, *Fire Saf. J.* 33 (1999) 115–128. [https://doi.org/10.1016/S0379-7112\(99\)00018-1](https://doi.org/10.1016/S0379-7112(99)00018-1).
- [18] X. Dai, A. Gamba, C. Liu, J. Anderson, M. Charlier, D. Rush, S. Welch, An engineering CFD model for fire spread on wood cribs for travelling fires, *Adv. Eng. Softw.* 173 (2022) 103213. <https://doi.org/10.1016/j.advengsoft.2022.103213>.
- [19] M. Autengruber, M. Lukacevic, G. Wenighofer, R. Mauritz, J. Füssl, Finite-element-based concept to predict stiffness, strength, and failure of wood composite I-joint beams under various loads and climatic conditions, *Eng. Struct.* 245 (2021) 112908. <https://doi.org/10.1016/j.engstruct.2021.112908>.
- [20] B.M. Suleiman, J. Larfeldt, B. Leckner, M. Gustavsson, Thermal conductivity and diffusivity of wood, *Wood Sci. Technol.* 33 (1999) 465–473. <https://doi.org/10.1007/s002260050130>.
- [21] K. Radmanović, I. Đukić, S. Pervan, Specific Heat Capacity of Wood, *Drv. Ind.* 65 (2014) 151–157. <https://doi.org/10.5552/drind.2014.1333>.
- [22] J. König, Effective thermal actions and thermal properties of timber members in natural fires, *Fire Mater.* 30 (2006) 51–63. <https://doi.org/10.1002/fam.898>.
- [23] J. Pailhes, C. Pradere, J.-L. Battaglia, J. Toutain, A. Kusiak, A.W. Aregba, J.-C. Batsale, Thermal quadrupole method with internal heat sources, *Int. J. Therm. Sci.* 53 (2012) 49–55. <https://doi.org/10.1016/j.ijthermalsci.2011.10.005>.
- [24] P. Santos, J.R. Correia, L. Godinho, A.M.P.G. Dias, H. Craveiro, Experimental and numerical assessment of a cross-insulated timber panel solution, *Eng. Struct.* 235 (2021) 112061. <https://doi.org/10.1016/j.engstruct.2021.112061>.
- [25] D. Maillet, *Thermal quadrupoles: solving the heat equation through integral transforms*, 1st ed., Wiley, Chichester; New York, 2000.
- [26] J.J. Moré, The Levenberg-Marquardt algorithm: Implementation and theory, in: *G.A. Watson (Ed.), Numer. Anal., Springer, Berlin, Heidelberg, 1978: pp. 105–116.* <https://doi.org/10.1007/BFb0067700>.
- [27] E. Donval, D. Toan Pham, G. Hassen, P. de Buhan, D. Pallix, A numerical homogenization method for the determination of the thermal bowing of a masonry wall exposed to fire: Application to natural stone masonry, *Eng. Struct.* 266 (2022) 114541. <https://doi.org/10.1016/j.engstruct.2022.114541>.

(2022) ; <http://www.jmaterenvirosci.com>